ABSTRACT: Titin, an elastic and giant myofibrillar protein, is responsible for generating passive tension and maintaining sarcomere structure in striated muscles. Several studies have reported attenuation of passive tension and disorganization of sarcomere in atrophic muscles, but the changes of titin have not been investigated after denervation. For this purpose, we used sodium dodecyl sulfate–polyacrylamide gel electrophoresis (SDS-PAGE) and immunofluorescent staining to examine titin in innervated and denervated tibialis anterior (TA) muscles of the rat. With increasing denervation time, we found a greater loss of titin than myosin heavy chain (MHC) and actin contents in atrophic TA muscle. The ratios of titin/MHC and titin/actin gradually decreased following denervation. In contrast, ratios of MHC/actin in the denervated groups showed no significant differences with the controls even at 56 days postdenervation. The ultrastructure of myofibrils also showed disturbed arrangements of myofilaments and a disorganized contractile apparatus in denervated muscle. Immunofluorescent staining displayed translocation of the titin epitope from the Z-line to the I-band, suggesting that the apparent cleavage of titin occurred near the Z-line region during the atrophying process. Our study provides evidence that titin is more sensitive to degradation than MHC and actin after denervation. Moreover, the titin decline results in the loss of titin-based sarcomeric integrity in atrophic muscle.

Muscle Nerve **32:** 798–807, 2005

DECLINE IN TITIN CONTENT IN RAT SKELETAL MUSCLE AFTER DENERVATION

SY-PING CHEN, MS,[1,2] JOEN-RONG SHEU, PhD,[1,3] AMING CHOR-MING LIN, MD,[4] GEORGE HSIAO, PhD,[3] and TSORNG-HARN FONG, PhD[5]

[1] Graduate Institute of Medical Sciences, Taipei Medical University, Taipei, Taiwan
[2] Department of Nursing, Chang-Gung Institute of Technology, Taoyuan, Taiwan
[3] Department of Pharmacology, Taipei Medical University, Taipei, Taiwan
[4] Emergency Department, Shin Kong Wu Ho-Su Memorial Hospital, Taipei, Taiwan
[5] Department of Anatomy, Taipei Medical University, 250 Wu-Hsing Street, Taipei 110, Taiwan

Accepted 28 July 2005

Titin (also known as connectin) is a giant elastic protein (3,000–4,000 kDa) and the third most abundant muscle protein after myosin and actin in skeletal and cardiac muscle cells.[24,37] In the sarcomere, titin molecules span the entire 1–2-μm distance from the Z-line to the M-line.[6,12] The human titin gene is located on chromosome 2q31 and contains 363 exons encoding 38,138 amino acid residues,[2] and different exon-skipping pathways produce titin transcripts that code for different titin isoforms.[10,27]

The elasticity of skeletal muscle titin originates in the I-band region, which consists of three major domains: the tandem immunoglobulin-like domain; a unique sequence rich in proline (P), glutamate (E), valine (V), and lysine (K) residues termed the "PEVK" domain; and the N2A domain.[12,27] Conformational studies have documented that the PEVK domain has two major motifs, i.e., PPAK and poly-E motifs,[13] and three malleable conformational states, i.e., a polyproline II helix, a beta turn, and an unordered coil. [23] Furthermore, the poly-E motifs of the PEVK domain were found to cause titin to act as a calcium-dependent molecular spring that stabilizes the muscle during contraction.[20] Recent studies have revealed that some skeletal muscles coexpress longer ($N2A_L$) and shorter ($N2A_S$) titin isoforms, also at the single-fiber level; variations in the overall $N2A_L$:

Abbreviations: DMD, Duchenne muscular dystrophy; EDL, extensor digitorum longus muscle; EDTA, ethylenediaminetetraacetic acid; FCMD, Fukuyama-type congenital muscular dystrophy; MGT, myasthenia gravis and thymoma; MHC, myosin heavy chain; ODI, optical density integral; PEVK, proline (P), glutamate (E), valine (V), and lysine (K); PMSF, phenylmethylsulfonyl fluoride; SDS-PAGE, sodium dodecyl sulfate–polyacrylamide gel electrophoresis; TA, tibialis anterior muscle; TMD, tibialis muscular dystrophy

Key words: denervation; muscle atrophy; myofibrillar protein; skeletal muscle; titin

Correspondence to: T.-H. Fong, e-mail: thfong@tmu.edu.tw

Published online 20 September 2005 in Wiley InterScience (www.interscience.wiley.com). DOI 10.1002/mus.20432

$N2A_S$ ratio may add to the fine-tuning of titin-stiffness in the entire muscle.[27]

The distinct titin I-band spring elements appear to be recruited in a sequential order. The tandem immunoglobulin repeats first extend as the sarcomere is stretched at low forces. Subsequently, the PEVK domain unravels only upon reaching sufficiently high external forces.[6,12] In addition to the elasticity generated by the I-band titin region, the A-band titin segment is strongly associated with myosin filaments, so it keeps the thick filaments in a centered position and avoids misalignment of the sarcomeres. At the Z-line, the N-terminal end of titin is capped by telethonin and interacts with actin and α-actinin via Z-repeat domains. At the M-line, the C-terminal end of titin interacts with myomesin.[6] Taken together, titin behaves as a molecular spring whose extensible properties greatly contributes to the passive tension of myofibrils and maintains the structural and functional stability of sarcomeres.

Cutting of the sciatic nerve is a well-developed denervation model to induce muscle atrophy.[3,9,14,19,22,30] After denervation, skeletal muscles undergo myocyte apoptosis, a reduction in single-fiber cross-sectional areas, misalignment of sarcomeres, and changes in contractile properties. In general, irreversible muscle atrophy develops, and the denervated muscle does not regain contractile function in long-term denervation.[32] In addition, muscle pathological analyses have revealed that titin may be implicated in several muscular diseases, such as Duchenne muscular dystrophy (DMD),[25] Fukuyama-type congenital muscular dystrophy (FCMD),[26] myasthenia gravis and thymoma (MGT),[29] and tibialis muscular dystrophy (TMD).[15] However, the exact relationship between denervation-induced muscle atrophy and the changes of titin is unclear.

The purpose of this study was to quantify the contents of titin, myosin heavy chain (MHC), and actin by sodium dodecyl sulfate–polyacrylamide gel electrophoresis (SDS-PAGE) and densitometric analysis by using denervation-induced hindlimb atrophy. The ratios of titin to MHC (titin/MHC), titin to actin (titin/actin), and MHC to actin (MHC/actin) were also calculated. In addition, the ultrastructure of sarcomere and changes of the titin epitope near the Z-line were examined by electron microscopy and immunofluorescence, respectively.

MATERIALS AND METHODS

Animals and Surgical Procedures. Surgery was performed on adult male Wistar rats (6 weeks old, 200–250 g) under chloral hydrate anesthesia. The unilateral right hindlimb was denervated by excision of 8–10 mm of the sciatic nerve and the contralateral left leg served as a control without nerve sectioning. After denervation, atrophy of the right leg muscles was allowed to progress for 0 ($n = 6$), 7 ($n = 18$), 28 ($n = 32$), and 56 ($n = 38$) days, respectively. This study was approved by the Animal Care Committee of the Taipei Medical University.

Sample Preparation. At the stated postdenervation times, animals were euthanized and sacrificed with an intraperitoneal injection (80 mg/kg) of sodium pentobarbital (MTC Pharmaceuticals, Cambridge, Ontario, Canada). The tibialis anterior (TA) muscles were dissected out from both the right (denervated) and the left (innervated) legs and weighed. Subsequently, muscles were immediately snap-frozen in liquid nitrogen, and samples were prepared for SDS-PAGE analysis.[28] Frozen muscles were pulverized to a fine powder in liquid nitrogen using a mortar and pestle, and the tissue powders were homogenized in a Teflon/glass homogenizer in ice-cold lysis buffer (5 mM ethylenediaminetetraacetic acid, EDTA; 30 μg/ml leupeptin; 100 μg/ml phenylmethylsulfonyl fluoride, PMSF; and 20 mM Tris-base; pH 7.5) on ice. We used the same weight to volume dilution (1 mg muscle tissue/15 μl of lysis buffer). Also, the total content of protein in the myofibrils was measured with a protein assay kit (Bio-Rad, Hercules, California), and the concentration was adjusted to 4 mg/ml with ice-cold lysis buffer. Subsequently, myofibrils were solubilized with an equal volume of 2× SDS sample buffer (2 mM EDTA, 2% SDS, 1.2 M β-mercaptoethanol, 20% glycerol, 0.02% bromophenol blue, and 20 mM Tris-base; pH 8.0) and heated to 50°C for 20 min.[5]

Gel Electrophoresis. A step gradient minigel with an ambiguous interface was made by the improved method of Chen and coworkers.[5] To determine the optical loading volume and assure working within the linear range of the system, a loading range of each sample was electrophoresed on a "calibration gel" as described previously.[1,33] After electrophoresis, the gel slabs were stained with Coomassie brilliant blue R-250. Densitometric analysis was performed with a Photo-Print Digital Imaging System (IP-008-SD; Vilber Lourmat, Marne-la-Vallée, France) with analytic software (Bio-1D Light, V 2000). The optical density integrals (ODIs) of total titin (T1+T2), MHC, and actin were measured for each loading volume, and the slope of the relationship between ODI and loading volume was determined by linear regression analysis. The ratios of

titin/MHC and titin/actin were calculated as the slope of the total titin ODI/loading volume divided by the slope of MHC ODI/loading volume and the slope of actin ODI/loading volume, respectively. The ratio of MHC to actin was calculated as the slope of MHC ODI/loading volume divided by the slope of actin ODI/loading volume. The HiMark unstained high-molecular-weight protein standard (Invitrogen, Carlsbad, California) served as a reference band to ensure accurate molecular weight identification.

Immunoblot Analysis. For immunoblot analysis, gels were electroblotted onto nitrocellulose paper.[5] After blocking, the membrane was reacted with the primary antibodies of mouse anti-titin (T12) monoclonal antibody (Boehringer Mannheim, Indianapolis, Indiana) and the primary antibody was omitted in the negative control. After washing, the strips were incubated with biotin-conjugated rat serum-adsorbed, and affinity-purified secondary antibody (Vector, Burlingame, California). Following washing, peroxidase-conjugated streptavidin (Dako, Glostrup, Denmark) was added. Subsequently, positive bands were visualized using hydrogen peroxide as the substrate and diaminobenzidene as the chromogen.

Electron Microscopy. To investigate the effect of denervation on the morphological characteristics of myofibrils, we observed the ultrastructural changes between innervated and denervated myofibrils using electron microscopy. Under chloral hydrate anesthesia, the 56-day denervated rats were perfused from the left ventricle of the heart with normal saline and then a mixed aldehyde solution composed of 2% paraformaldehyde and 2% glutaraldehyde in 0.1 M phosphate buffer (pH 7.4). The TA muscles were removed and postfixed in the same fixative for 4 h at 4°C. Subsequently, the samples were cut longitudinally with the knife-edge parallel to the muscle fiber and osmicated using 1% osmium tetroxide in 0.1 M cacodylate buffer (pH 7.2). Samples were dehydrated in an ethanol series and embedded in Epon 812 using standard procedures. Ultrathin sections were cut and double-stained with uranyl acetate and lead citrate, and then examined in a Hitachi H-600 electron microscope (Hitachi, Tokyo, Japan).

Immunofluorescence. Myofibrils were prepared for immunofluorescence staining according to Wang and Greaser with some modifications.[38] Briefly, the hindlimb was cut from the middle of the femur bone; the origin and insertion of the TA muscles were retained. The muscles were explored by removing the skin and connective fascia and incubated with ice-cold rigor buffer (75 mM KCl, 2 mM $MgCl_2$, 2.5 mM EDTA, 0.1 mM PMSF, and 10 mM Tris-base; pH 6.8) containing 0.5% Triton X-100 at 4°C overnight. In order to rapidly obtain abundant single myofibrils, the TA muscles of both innervated and denervated groups were homogenized in ice-cold rigor buffer with a stainless steel polytron (PT 1200; Kinematica, Littau/Luzern, Switzerland) for 15 s on ice. This myofibril purification was performed in rigor buffer to conserve the structure of sarcomeres.

Indirect immunofluorescence staining of myofibrils followed reported procedures.[4] The myofibrils were placed on poly-L-lysine–coated glass slides for adhesion, fixed with 10% formalin in rigor buffer, and then blocked with 5% nonfat milk. Subsequently, the myofibrils were reacted with a mouse anti-titin (T12) monoclonal antibody. After washing, samples were incubated with a fluorescein isothiocyanate-labeled goat anti-mouse secondary antibody (Sigma, St. Louis, Missouri), mounted with mounting medium (2% n-propyl gallate and 50% glycerol in phosphate-buffered saline; pH 8.0), and examined with a Nikon epifluorescence microscope (Nikon, Tokyo, Japan).

Statistical Analysis. Values are expressed as the mean ± SEM. Student's paired *t*-test was used to verify the significance of differences between denervated and innervated muscles. At all times, a *P*-value of less than 0.05 was considered significant.

RESULTS

Decrease in Muscle Weight following Denervation. TA muscles taken from the right (denervated) and left (innervated) legs were weighed at 0, 7, 28, and 56 days postdenervation. A gradual reduction in denervated muscle mass was observed in contrast to the innervated muscle mass. Alterations of mean muscle mass after denervation were expressed in percentages relative to the mean mass of the corresponding contralateral, innervated muscle of each rat. After 7 days of denervation, the weight of the denervated TA muscle had decreased to 75.1% compared with the contralateral one. On subsequent days, the TA muscle had decreased to approximately 30.4% and 15.6% of the innervated groups on days 28 and 56 postdenervation, respectively. Thus, the muscle mass rapidly decreased during the first 28 days, and thereafter slowly decreased until day 56 postdenervation. Changes in muscle mass were used as a criterion of denervation-induced muscle atrophy.

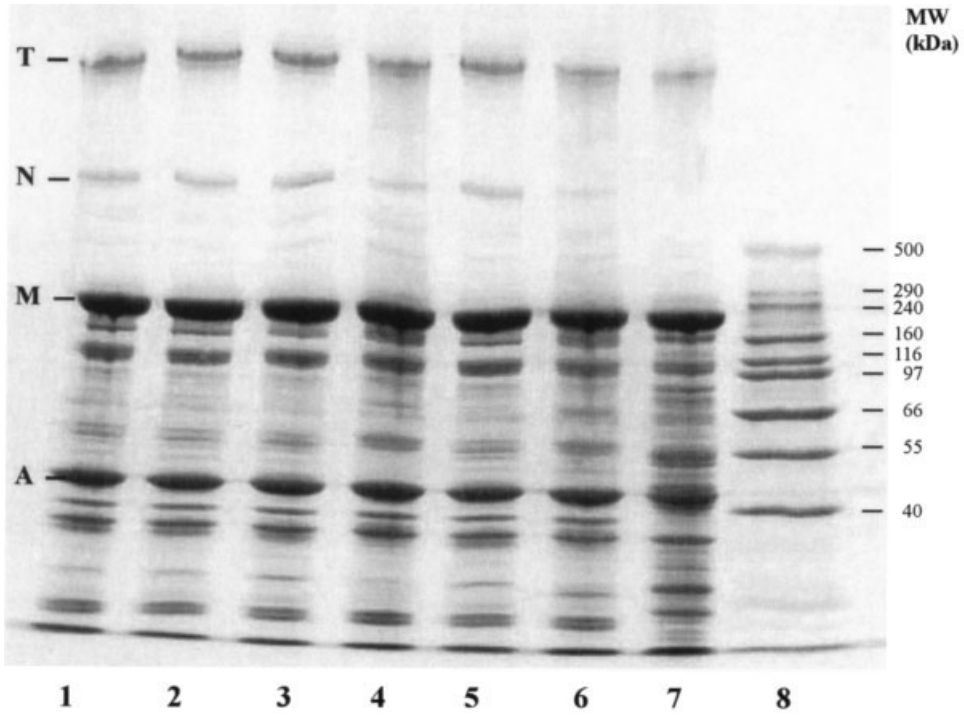

FIGURE 1. SDS-PAGE analysis of myofibrillar proteins from rat TA muscles after denervation. The gel was stained with Coomassie brilliant blue R-250. Lanes 1 and 2, 3 and 4, and 5 and 6, innervated and denervated myofibrillar proteins, respectively, on days 7, 28, and 56 after denervation. Lane 7, rat cardiac muscles, included as a titin migration reference. Lane 8, high-molecular-weight protein standard. Myosin and actin were abundant in innervated and denervated myofibrils. Titin had apparently decreased on days 28 and 56 after denervation (the highest bands in lanes 5 and 7). T, titin; N, nebulin; M, myosin heavy chain; A, actin.

Decrease in Titin Content following Denervation. SDS-PAGE was performed to separate the myofibrillar proteins in innervated and denervated TA muscles. Approximately 5 μg of protein was loaded in each lane, but greater emphasis was placed on equal loading of each lanes. The highest titin doublet (3,000–4,000 kDa), nebulin (~800 kDa), and abundant MHC (220 kDa) and actin (42 kDa) were all visible in Coomassie brilliant blue–stained gels of innervated muscles (Fig. 1, lanes 1 to 6). The MHC and actin contents of denervated groups were similar to those of the innervated groups. However, the titin contents in the denervated groups had apparently decreased, especially on days 28 and 56 following denervation (top bands in lanes 4 and 6 of Fig. 1). The gel profile of the left ventricular muscle of rat heart was included as a reference of titin migration, and the total amount of titin was less abundant in cardiac muscle compared with skeletal muscle (Fig. 1, lane 7). In addition, a single band of nebulin was present in skeletal muscles (Fig. 1, lanes 1 to 6) but not in cardiac muscle (Fig. 1, lane 7).

Immunoblot analysis confirmed that the highest bands on top of the gel were recognized by the anti-titin (T12) monoclonal antibody (Fig. 2A). The density of the highest band in denervated muscle was weaker than that in innervated muscle on day 56 postdenervation. Nonspecific binding bands of the secondary antibody near the bottom of the papers

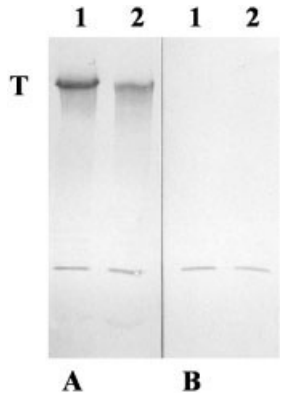

FIGURE 2. Western blot analysis of myofibrillar proteins of innervated and denervated TA muscles with anti-titin (T12) monoclonal antibody, respectively, confirming the titin. **(A)** Immunoblot with the T12 monoclonal antibody; **(B)** primary antibody blank control. Lanes 1 and 2, innervated and denervated myofibrillar proteins, respectively, on day 56 after denervation. Note the difference in titin content between the innervated and denervated samples. The titin content had obviously decreased following denervation. Nonspecific binding bands can be seen near the bottom of the papers. T, titin.

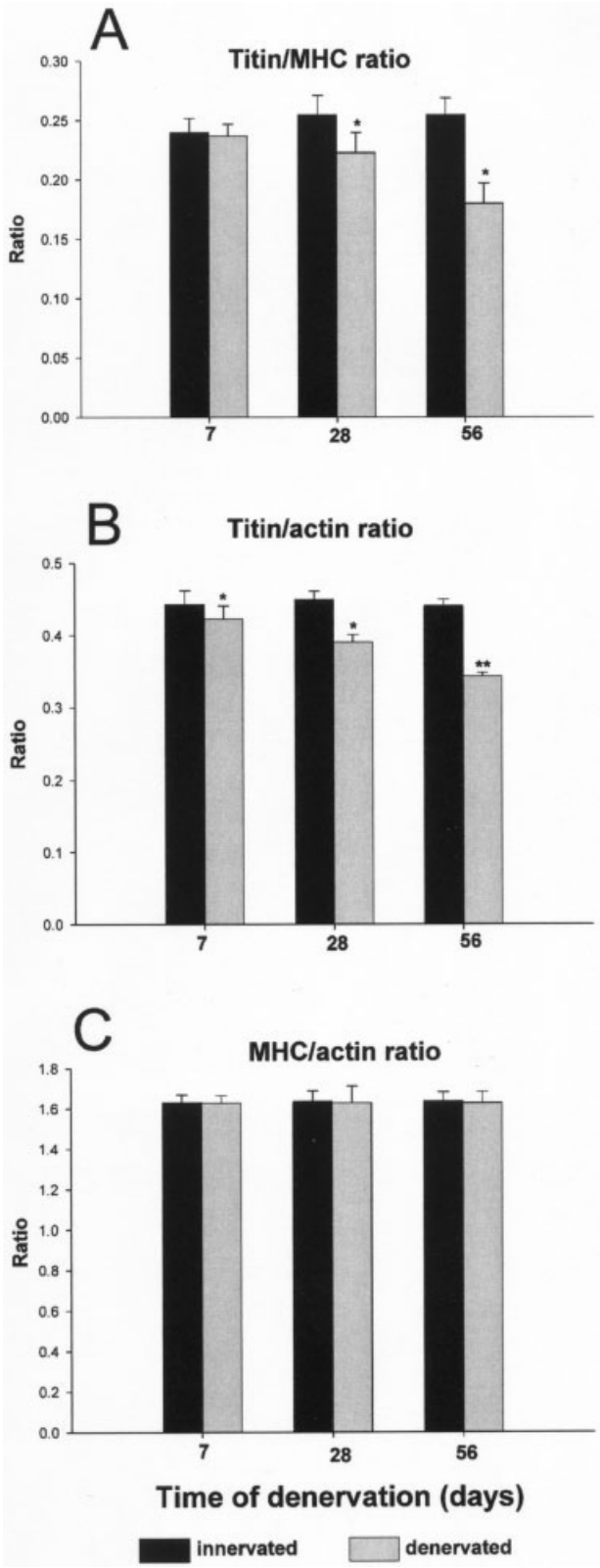

FIGURE 3. Effects of denervation on the ratios of titin/MHC **(A)**, titin/actin **(B)**, and MHC/actin **(C)**. Titin, MHC, and actin contents. Ratios are presented as mean ± SEM. $^{*}P < 0.05$ and $^{**}P < 0.01$ represent significant differences as compared to the paired innervated group. The titin/MHC and titin/actin ratios gradually decreased, but the MHC/actin ratio showed no significant difference with the innervated group following denervation.

were also seen in the primary antibody blank control (Fig. 2B). Titin doublet bands in the gels were highly repeatable and were identified by migration patterns and immunoblot analysis. These data showed obvious decline in titin content in denervation-induced atrophic muscle.

Larger Loss of Titin than MHC and Actin. The contents of titin, MHC, and actin in denervated and innervated TA muscles were evaluated, and the relative proportions were calculated by quantitative densitometry as described earlier. Quantitative analysis by linear regression between the ODI and loading volume showed that the slopes of the ODI/loading volume of titin were 22,872 ± 1,436, 24,683 ± 1,029 and 23,644 ± 1,231 in innervated muscles on days 7, 28, and 56, respectively. Following denervation, the slopes of the ODI/loading volume of titin decreased to 21,932 ± 1,522, 21,438 ± 874, and 18,069 ± 684 in denervated muscles on days 7, 28, and 56. Therefore, total titin contents in denervated muscles had significantly decreased to about 95.9%, 86.8%, and 76.4% of innervated groups on days 7, 28, and 56 postdenervation, respectively.

The ratios of titin to MHC (titin/MHC) had decreased to 98.8%, 87.4%, and 70.6% of the control groups on days 7, 28, and 56 postdenervation, respectively (Fig. 3A). The ratios of titin to actin (titin/actin) had also decreased to 95.5%, 86.9%, and 77.8% of the control groups on days 7, 28, and 56 postdenervation, respectively (Fig. 3B). Decline of titin became more pronounced with time following denervation. However, the total MHC content decreased in parallel to the total actin content in denervated TA muscle, so the ratio of MHC to actin (MHC/actin) decreased only negligibly (Fig. 3C). These data revealed various degrees of decrease in myofibrillar proteins after denervation. Moreover, the amount of titin decreased more obviously than those of MHC and actin in denervated muscle.

Effects of Denervation on the Ultrastructure of Myofibrils. Organized sarcomeres and striations of the A-band, I-band, Z-line, M-line, and H-zone could clearly be observed in innervated muscle by electron microscopy (Fig. 4A). Mitochondria between myofibrils were abundant and intact. The triad containing terminal cisternae of sarcoplasmic reticulum and T-tubule was located at the A–I junction (Fig. 4B).

As the postdenervation time progressed, atrophy of muscle cells became prominent, but the degree of atrophy was not consistent among all muscle cells. Some muscle cells still contained well-ordered arrays of myofilaments even on day 56 of denervation (Fig.

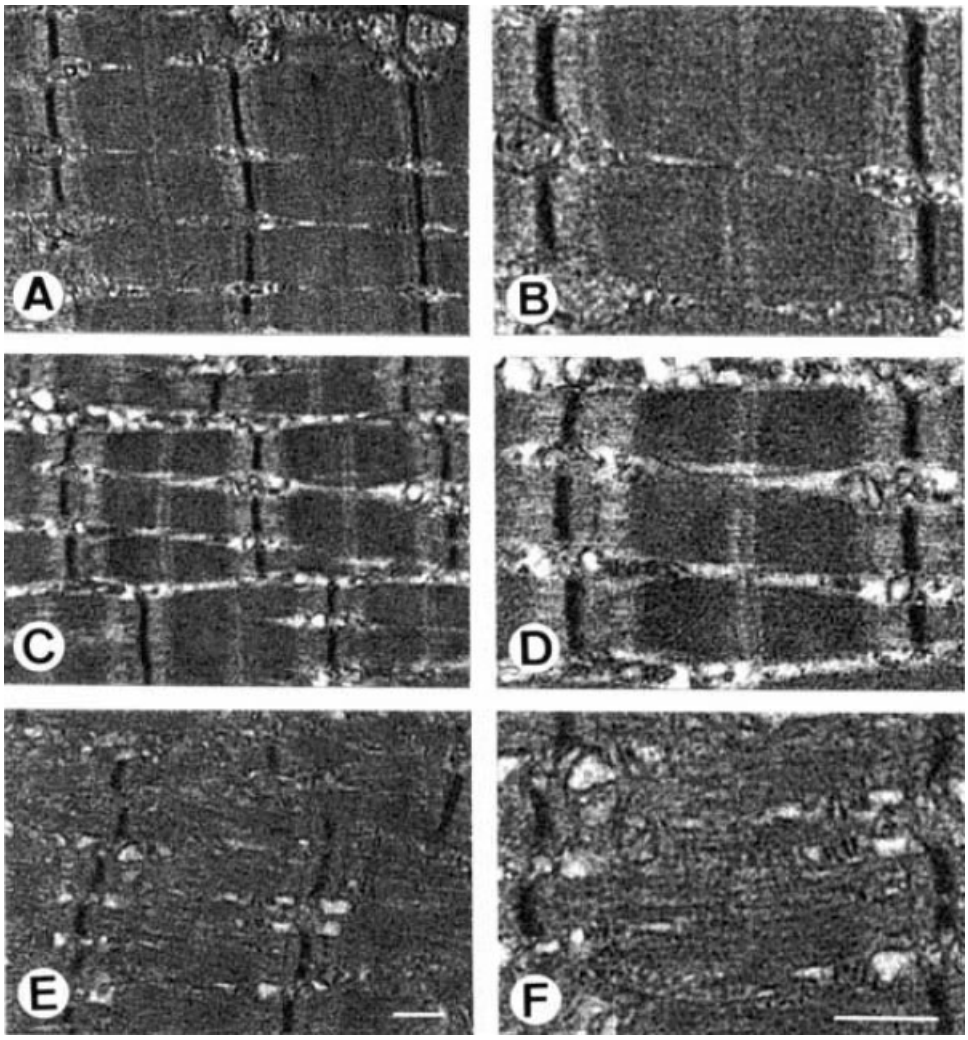

FIGURE 4. Electron micrographs of longitudinal sections through day 56–innervated and denervated muscles. **(B)**, **(D)**, and **(F)** are higher magnification micrographs of **(A)**, **(C)**, and **(E)**, respectively. **(A, B)** Electron micrographs of innervated muscle. The striations were evident, mitochondria between myofibrils were abundant, and the triads were located at the A–I junction. **(C, D)** Electron micrographs of denervated muscle. The remaining intact sarcomeres and striations were observed in some denervated muscle cells. Sarcoplasmic reticula were proliferated and extended in these denervated groups. **(E, F)** Electron micrographs of denervated muscle. Myofilaments disorganization was distinct and only the Z-line could be identified in most denervated muscle cells. The sarcomeres and sarcoplasmic reticulum became more disorganized. Bar, 0.5 μm.

4C). Striations of the A-band, I-band, Z-line, M-line, and H-zone were identified in these well-ordered sarcomeres. The proliferated and extended sarcoplasmic reticulum was observed between myofibrils in denervated muscle cells (Fig. 4D). In contrast, in most denervated muscle fibers containing disorganized sarcomeres, the mitochondria became smaller and fewer in number (Fig. 4E). The sarcoplasmic reticulum and triad became more expanded and disorganized. Several autophagic vesicles were scattered among the cytoplasm of denervated muscle fibers. The Z-lines could still be observed, but they were more irregular than those in innervated muscle (Fig. 4F). Following denervation, most muscle fibers contained a disorganized arrangement of the contractile apparatus. The disorganized sarcomeres indicated that the role of titin in stabilizing the sarcomeres was affected by denervation. In addition, the amount of endomysial collagen increased prominently around the denervated muscle fibers.

Effects of Denervation on Immunofluorescent Staining of Myofibrils. To examine changes in the titin epitope near the Z-line during denervation, we isolated individual myofibrils from muscles for immu-

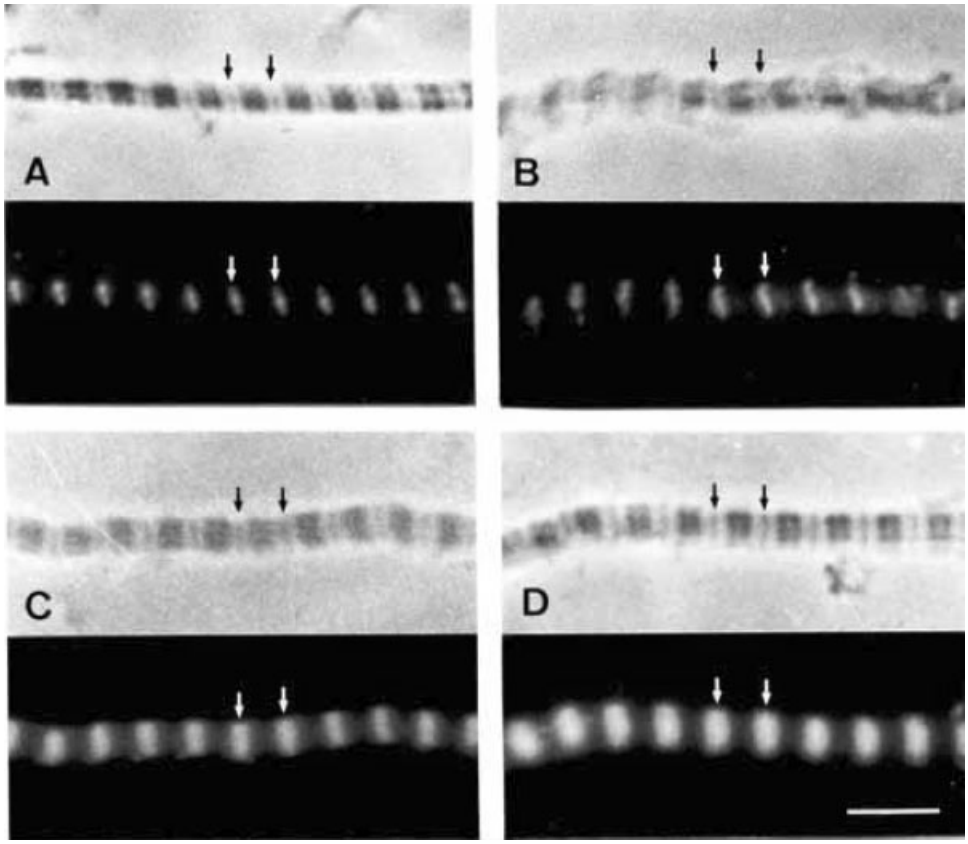

FIGURE 5. Phase-contrast and corresponding immunofluorescence micrographs of innervated and denervated myofibrils decorated with an anti-titin (T12) monoclonal antibody. In each pair of micrographs, the upper panel is the phase-contrast photograph, and the lower panel is the corresponding fluorescence picture. **(A)** Myofibril from innervated muscles on day 7; **(B)** myofibril from denervated muscles on day 7; **(C)** intact myofibril from denervated muscles on day 28; **(D)** intact myofibril from denervated muscles on day 56. Note the widening of fluorescence around the Z-line in the intact myofibrils of denervated muscles on days 28 and 56. Arrows indicate the positions of the Z-lines. Bar, 5 μm.

nofluorescence staining. Statistical analyses were performed to verify the appearances of myofibrils on photo fields. The phase-contrast profiles indicated that most of the isolated myofibrils (about 97.5%) from innervated muscle displayed an ordered structure of sarcomeres during the entire period of observation. The distinct striations of the A-band, I-band, Z-line, and H-zone could be identified in innervated myofibrils on day 7 (Fig. 5A, upper panel). Immunofluorescence of the anti-titin (T12) monoclonal antibody, which labels a titin epitope near the Z-line, exhibited an intense single band and periodic pattern at the Z-line of innervated myofibrils on day 7 (arrows in Fig. 5A, lower panel). The same morphology and staining pattern were also observed in innervated myofibrils on days 28 and 56.

At 7 days postdenervation, most denervated myofibrils (87.5%) remained as intact as the innervated myofibrils, but a few myofibrils (12.5%) had an irregular appearance (Fig. 5B, upper panel). Immunofluorescent staining of these irregular myofibrils still occurred at the Z-line with the T12 antibody in denervated myofibrils (arrows in Fig. 5B, lower panel).

At 28 days postdenervation, most denervated myofibrils had broken up after polytron treatment. Some remaining intact myofibrils were shorter than those isolated from innervated muscles. The numbers of remaining intact myofibrils were about four to five on each photograph. Striations of the A-band, I-band, and Z-line were observed in the remaining intact denervated myofibrils (Fig. 5C, upper panel). However, widening of the fluorescence around the Z-line was observed and indicated that the T12 epitope had shifted from the Z-line to the I-band (Fig. 5C, lower panel). Trombitás and colleagues have provided evidence that near the Z-line, titin is attached under tension.[35] Therefore, the translocation of T12 epitope might result from the loss of tension.

At 56 days postdenervation, most of the isolated myofibrils from denervated muscles had become dispersed. There were about one or two myofibrils remaining intact on each photograph. Striations of the A-band, I-band, and Z-line were still visible in the remaining intact denervated myofibrils (Fig. 5D, upper panel). The widening of the fluorescence around the Z-line was observed in the remaining intact myofibrils (Fig. 5D, lower panel). Immunofluorescent staining of the T12 epitope revealed that increasing denervation time might result in the apparent cleavage of titin near the Z-line region or the translocation of the ends of some of the titin molecules.

DISCUSSION

Our results demonstrate the progressive loss of muscle mass after sciatic nerve transection. The muscle mass rapidly declined within 28 days after denervation, and then slowly decreased during the remaining period of observation. These data are consistent with numerous previous reports.[8,14,18,19] Denervation-induced atrophy of skeletal muscle is associated with apoptosis of muscle cells. Several apoptotic events such as the upregulation of bax and bcl-2, activation of caspase, and fragmentation of DNA have been detected in denervated skeletal muscle.[32] As apoptosis progresses, the muscle mass gradually decreases in a time-dependent manner.

Using SDS-PAGE and densitometric analysis, myofibrillar proteins (such as titin, nebulin, MHC, and actin) decreased following denervation, but the degree of decrease was not equal among these myofibrillar proteins. The ratios of titin/MHC and titin/actin decreased, indicating that titin declined more rapidly and to a greater extent than either MHC or actin. This finding is similar to results of Toursel and coworkers, who reported a decrease of titin content in atrophic soleus after hindlimb unloading.[33]

However, MHC and actin decreased in parallel, so the MHC/actin ratio remained similar to that of the controls. Jakubiec-Puka reported that the MHC/actin ratio of the rat extensor digitorum longus (EDL) muscle was also maintained for about 1 month after denervation, but the ratio decreased in the latter stage of atrophy.[19] In our study, the MHC/actin ratio of TA muscle did not significantly differ from that of the controls even at 56 days postdenervation. The presented differences between TA and EDL muscles reflect the probable different sizes and atrophic degrees of the muscles.

Immunoblot analysis indicated that titin might have broken down or been cleaved in denervation-induced atrophying muscle. However, the mechanism of the downregulation of titin is unclear. Further studies are required to investigate why the content of titin more obviously declined than those of MHC and actin. Recently, calpains (calcium-activated cysteine proteases) were reported to mediate muscle protein degradation and participate in protein turnover in skeletal muscle.[7,17] Previous studies indicated that denervation enhanced calpain activities in rodent skeletal muscles.[8,18] In addition, activated calpains can digest titin, nebulin, and desmin,[7] but not MHC or actin.[34] Therefore, it seems likely that calpains are involved in the gradual loss in titin contents during denervation processes. Further studies will be necessary to clarify the relationship between titin changes and the calpain proteolytic system following denervation.

Ultrastructural observations revealed that muscle cells containing highly disorganized myofilaments of sarcomeres increased with increasing denervation time. These morphological observations are consistent with previous studies.[19,22,31] Several unique structural properties have established titin filaments as a crucial component of sarcomeric integrity of striated myofibrils.[6] Based on the morphological data, we speculated that the disorganized arrangement of contractile filaments might have resulted from the denervation-induced reduction in titin. However, different degrees of atrophy of muscle cells were also seen in denervated muscle. There were still some well-ordered sarcomeres even at 56 days postdenervation. This result is consistent with the observations of Lu and coworkers.[22] Striations of the A-band, I-band, Z-line, M-line, and H-zone were still identified in these ordered sarcomeres of denervated muscles, but not as clearly as those of the innervated groups. Several studies have confirmed the association of titin filament with thin filament in the I-band.[21,35,36,39] Yamasaki and coworkers have also shown that the PEVK domain of titin bound to thin filament in the I-band both in cardiac and skeletal muscle.[39] Therefore, titin might be cleaved but still bind to the thin filament, so the well-ordered sarcomere can maintain its ultrastructure in denervated muscles. During myofibril preparation for immunofluorescence, we also found that the well-ordered myofibrils in denervated muscles were resistant to polytron treatment.

Immunofluorescence staining with an anti-titin (T12) antibody demonstrated that the T12 epitope had translocated but remained in the Z-line and I-band of well-ordered myofibrils in denervated muscles. According to previous investigations, titin might bind firmly to the thin filament between the Z-line and N1

line, but be only weakly associated with the thin filament in the rest of the I-band.[21,36] Thus, as cleavage of titin near the Z-line occurred, titin tension might move the T12 epitope into the I-band and result in widening of the fluorescence around the Z-line as our data showed. Boyer-Berri and Greaser studied the effect of postmortem storage on the Z-line region of titin in bovine muscle and found a similar translocation of the titin epitope (FE-RE epitope). They suggested that the cleavage of titin might increase misalignment of the myofibrils and improve the tenderness of bovine muscles during postmortem storage.[4]

Physiological examinations of denervation-induced atrophic muscles have indicated the attenuation in force output, an increase in twitch times to peak, and elongation of half-relaxation times.[9,14] Although multiple factors may be involved, we suggest that the decline in titin might be a potential factor resulting in disorganized sarcomeres that would affect the interaction of myofilaments and contractile function. Nevertheless, the correlation between the reduction in titin content and the prolongation of half-relaxation times of atrophic muscle has not been reported to our knowledge. This absence of previous investigations makes it difficult to hypothesize a potential mechanism that can explain our observations. We can only speculate that the denervation-induced decline in titin might result in attenuation of the restoring force, and hence may be a contributing factor in the elongation of the twitch half-relaxation time. More experiments are required to determine whether the reduction in titin in denervated muscle affects the half-relaxation time.

Titin is responsible for the major source for generation of the restoring force in striated muscle[16] and is the most obvious determinant of the intracellular component for passive elasticity.[11] Thus it is conceivable that the reduction in the amount of titin in denervated muscle attenuates the titin-based intracellular passive force. This opinion is consistent with previous investigations that showed a decrease in the amount of titin reduced passive tension in the soleus muscle after 14 days of hindlimb unloading.[33] Another source of passive tension in skeletal muscle is collagen, the most abundant extracellular matrix. Our ultrastructural observations found that the amount of collagen increased around the denervated muscle cells. Earlier investigations also showed that denervation was accompanied by an increased level of extracellular collagen.[22,30] Because collagens contribute to the elastic properties of passive tension, an accumulation of collagen may thus participate in the remodeling of the passive force in denervated muscles. However, intracellular desmin, the main intermediate filament in muscle cells, is also slightly reduced in denervated soleus muscle.[3] Because desmin contributes nothing or very little to passive tension development,[1,11] we speculated that the reduction in desmin insignificantly affects intracellular passive tension in comparison to that in titin after denervation.

Due to titin's essential role in maintaining the normal function of skeletal muscle, the titin molecule is a candidate for association with a number of muscle diseases. The degradation of titin might be involved in the pathogenesis of myofibrillar degeneration in DMD[25] and FCMD[26] using Western blot analysis. The serum concentration of titin autoantibodies was correlated with the severity of MGT, and their presence might predict an unsatisfactory outcome after thymectomy.[29] The mutation in the *TTN* gene, encoding the titin protein, causes a functional defect of the M-line titin, and titinopathy is considered to be the genesis of the TMD disease phenotype.[15] These studies support titin playing a crucial role in the sarcomeric cytoarchitecture and in multiple functions of skeletal muscle.

In conclusion, the most striking finding in the present study is a greater loss of titin than MHC and actin after denervation. The titin content declined and its cleavage near the Z-line region might have resulted in changes in the fluorescent staining pattern and misalignment of sarcomeres during the atrophying process. This study provides evidence that titin is more sensitive to degradation than MHC and actin after denervation. The titin changes may be related to misalignment of sarcomeres and reduction of passive tension in atrophic muscle.

This study was supported by research grants from the National Science Council of Taiwan (NSC 89-2314-B-038-033) and Shin Kong Wu Ho-Su Memorial Hospital (SKH-TMU-93-33). We thank Professor Wen-Mei Fu (National Taiwan University) for her helpful discussions of this manuscript.

REFERENCES

1. Anderson J, Joumaa V, Stevens L, Neagoe C, Li Z, Mounier Y, et al. Passive stiffness changes in soleus muscles from desmin knockout mice are not due to titin modifications. Pflugers Arch 2002;444:771–776.
2. Bang ML, Centner T, Fornoff F, Geach AJ, Gotthardt M, McNabb M, et al. The complete gene sequence of titin, expression of an unusual ≈700-kDa titin isoform, and its interaction with obscurin identify a novel Z-line to I-band linking system. Circ Res 2001;89:1065–1072.
3. Boudriau S, Côté CH, Vincent M, Houle P, Tremblay RR, Rogers PA. Remodeling of the cytoskeletal lattice in denervated skeletal muscle. Muscle Nerve 1996;19:1383–1390.
4. Boyer-Berri C, Greaser ML. Effect of postmortem storage on the Z-line region of titin in bovine muscle. J Anim Sci 1998; 76:1034–1044.

5. Chen SP, Sheu JR, Lai CY, Lin TY, Hsiao G, Fong TH. Detection of myofibrillar proteins using a step gradient minigel with an ambiguous interface. Anal Biochem 2005;338:270–277.
6. Clark KA, McElhinny AS, Beckerle MC, Gregorio CC. Striated muscle cytoarchitecture: an intricate web of form and function. Annu Rev Cell Dev Biol 2002;18:637–706.
7. Delgado EF, Geesink GH, Marchello JA, Goll DE, Koohmaraie M. Properties of myofibril-bound calpain activity in longissimus muscle of callipyge and normal sheep. J Anim Sci 2001; 79:2097—2107.
8. Elce JS, Hasspieler R, Boegman RJ. Ca^{2+}-activated protease in denervated rat skeletal muscle measured by an immunoassay. Exp Neurol 1983;81:320–329.
9. Finol HJ, Lewis DM, Owens R. The effects of denervation on contractile properties of rat skeletal muscle. J Physiol (Lond) 1981;319:81–92.
10. Freiburg A, Trombitás K, Hell W, Cazorla O, Fougerousse F, Centner T, et al. Series of exon-skipping events in the elastic spring region of titin as the structural basis for myofibrillar elastic diversity. Circ Res 2000;86:1114–1121.
11. Granzier HL, Irving TC. Passive tension in cardiac muscle: contribution of collagen, titin, microtubules, and intermediate filaments. Biophys J 1995;68:1027–1044.
12. Granzier HL, Labeit S. Cardiac titin: an adjustable multifunctional spring. J Physiol (Lond) 2002;541:335–342.
13. Greaser M. Identification of new repeating motifs in titin. Proteins 2001;43:145–149.
14. Gundersen K. Early effects of denervation on isometric and isotonic contractile properties of rat skeletal muscles. Acta Physiol Scand 1985;124:549–555.
15. Hackman P, Vihola A, Haravuori H, Marchand S, Sarparanta J, de Seze J, et al. Tibial muscular dystrophy is a titinopathy caused by mutations in *TTN*, the gene encoding the giant skeletal-muscle protein titin. Am J Hum Genet 2002;71:492–500.
16. Helmes M, Trombitás K, Granzier H. Titin develops restoring force in rat cardiac myocytes. Circ Res 1996;79:619–626.
17. Huang J, Forsberg NE. Role of calpain in skeletal-muscle protein degradation. Proc Natl Acad Sci USA 1998;95:12100–12105.
18. Hussain H, Dudley GA, Johnson P. Effects of denervation on calpain and calpastatin in hamster skeletal muscles. Exp Neurol 1987;97:635–643.
19. Jakubiec-Puka A. Changes in myosin and actin filaments in fast skeletal muscle after denervation and self-reinnervation. Comp Biochem Physiol [A] 1992;102:93–98.
20. Labeit D, Watanabe K, Witt C, Fujita H, Wu Y, Lahmers S, et al. Calcium-dependent molecular spring elements in the giant protein titin. Proc Natl Acad Sci USA 2003;100:13716–13721.
21. Linke WA, Ivemeyer M, Labeit S, Hinssen H, Rüegg JC, Gautel M. Actin–titin interaction in cardiac myofibrils: probing a physiological role. Biophys J 1997;73:905–919.
22. Lu DX, Huang SK, Carlson BM. Electron microscopic study of long-term denervated rat skeletal muscle. Anat Rec 1997;248: 355–365.
23. Ma K, Wang K. Malleable confirmation of the elastic PEVK segment of titin: non-co-operative interconversion of polyproline II helix, β-turn and unordered structures. Biochem J 2003;374:687–695.
24. Maruyama K, Matsubara S, Natori R, Nonomura Y, Kimura S, Ohashi K, et al. Connectin, an elastic protein of muscle: characterization and function. J Biochem 1977;82:317–337.
25. Matsumura K, Shimizu T, Nonaka I, Mannen T. Immunochemical study of connectin (titin) in neuromuscular diseases using a monoclonal antibody: connectin is degraded extensively in Duchenne muscular dystrophy. J Neurol Sci 1989;93: 147–156.
26. Matsumura K, Shimizu T, Sunada Y, Mannen T, Nonaka I, Kimura S, et al. Degradation of connectin (titin) in Fukuyama-type congenital muscular dystrophy: immunochemical study with monoclonal antibodies. J Neurol Sci 1990;98:155–162.
27. Neagoe C, Opitz CA, Makarenko I, Linke WA. Gigantic variety: expression patterns of titin isoforms in striated muscles and consequences for myofibrillar passive stiffness. J Muscle Res Cell Motil 2003;24:175–189.
28. Parr T, Sensky PL, Bardsley RG, Buttery PJ. Calpastatin expression in porcine cardiac and skeletal muscle and partial gene structure. Arch Biochem Biophys 2001;395:1–13.
29. Romi F, Skeie GO, Gilhus NE, Aarli JA. Striational antibodies in myasthenia gravis: reactivity and possible clinical significance. Arch Neurol 2005;62:442–446.
30. Salonen V, Lehto M, Kalimo H, Penttinen R, Aro H. Changes in intramuscular collagen and fibronectin in denervation atrophy. Muscle Nerve 1985;8:125–131.
31. Stonnington HH, Engel AG. Normal and denervated muscle: a morphometric study of fine structure. Neurology 1973;23: 714–724.
32. Tews DS. Apoptosis and muscle fibre loss in neuromuscular disorders. Neuromuscul Disord 2002;12:613–622.
33. Toursel T, Stevens L, Granzier H, Mounier Y. Passive tension of rat skeletal soleus muscle fibers: effects of unloading conditions. J Appl Physiol 2002;92:1465–1472.
34. Toyo-Oka T, Masaki T, Okamoto J, Tanaka T. Calcium-activated neutral protease from bovine ventricular muscle: isolation and some of its properties. J Mol Cell Cardiol 1979;11: 769–786.
35. Trombitás K, Granzier H. Actin removal from cardiac myocytes shows that near Z line titin attaches to actin while under tension. Am J Physiol 1997;273:C662–C670.
36. Trombitás K, Greaser ML, Pollack GH. Interaction between titin and thin filaments in intact cardiac muscle. J Muscle Res Cell Motil 1997;18:345–351.
37. Wang K, McClure J, Tu A. Titin: major myofibrillar components of striated muscle. Proc Natl Acad Sci USA 1979;76: 3698–3702.
38. Wang SM, Greaser ML. Immunocytochemical studies using a monoclonal antibody to bovine cardiac titin on intact and extracted myofibrils. J Muscle Res Cell Motil 1985;6:293–312.
39. Yamasaki R, Berri M, Wu Y, Trombitás K, McNabb M, Kellermayer MSZ, et al. Titin-actin interaction in mouse myocardium: passive tension modulation and its regulation by calcium/S100A1. Biophys J 2001;81:2297–2313.